

# Correlating Structure and Electronic Band-Edge Properties in Organolead

## Halide Perovskites Nanoparticles

Qiushi Zhu<sup>a</sup>, Kaibo Zheng<sup>b,c</sup>, Mohamed Abdellah<sup>b,f</sup>, Alexander Generalov<sup>d</sup>, Dörthe Haase<sup>d</sup>, Stefan Carlson<sup>d</sup>, Yuran Niu<sup>d</sup>, Jimmy Heimdal<sup>d</sup>, Anders Engdahl<sup>d</sup>, Maria E. Messing<sup>d</sup>, Tonu Pullerits<sup>b,†</sup>, Sophie E. Canton<sup>g,h,†</sup>

### Supporting information:

#### 1. Synthesis methods and characterization:

**Synthesis of precursors:** methylammonium (MA) bromide ( $\text{CH}_3\text{NH}_3\text{Br}$ ) and octylammonium (OTA) bromide ( $\text{CH}_3(\text{CH}_2)_7\text{NH}_3\text{Br}$ ) were synthesized by reaction of the corresponding amine in water/HBr accordingly to the previously reports. In brief, for ( $\text{CH}_3\text{NH}_3\text{Br}$ ) 36.9 ml of HBr and 83.4 ml of  $\text{CH}_3\text{NH}_2$  were stirred for two hours in ice bath. The resulting solution was evaporated until the formation of white crystals. The white crystals then were recrystallized from ethanol solution and then used as a precursor for  $\text{CH}_3\text{NH}_3\text{PbBr}_3$  colloidal nanoparticles. The same procedures were repeated in order to prepare ( $\text{CH}_3(\text{CH}_2)_7\text{NH}_3\text{Br}$ ) where 33.5 ml of  $\text{CH}_3(\text{CH}_2)_7\text{NH}_2$  and 22.6 ml of HBr were stirred for two hours in ice bath.

**Synthesis of  $\text{CH}_3\text{NH}_3\text{PbBr}_3$  bulk-like crystals:**  $\text{MAPbBr}_3$  microcrystals were prepared by spin coating  $\text{MAPbBr}_3$  precursors in DMF onto glass substrates with 2000 rpm for 30 sec. Substrates were then annealed in air at 85 °C for half an hour to form orange colored crystals. In order to verify the crystal size, different dilution of precursors (original,  $\times 2$ ,  $\times 4$ ,  $\times 8$ ,  $\times 16$ ,  $\times 25$ ) were used which produced crystals with mean size of 14.7, 6.2, 4.2, 2.0 and 0.4  $\mu\text{m}$ , respectively.

**Synthesis of  $\text{CH}_3\text{NH}_3\text{PbBr}_3$  colloidal nanoparticles:**  $\text{CH}_3\text{NH}_3\text{PbBr}_3$  colloidal nanoparticles were synthesized via hot injection of  $\text{MABr}$ / $\text{OTABr}$  and  $\text{PbBr}_2$  precursors in coordinator solvent analogous to previous reports. In brief, 0.5 mmol oleic acid in 10 ml of octadecene was stirred and heated at 80 °C followed by addition of 0.3 mmol  $\text{OTABr}$  in 1 ml DMF. Then 0.2 mmol of  $\text{MABr}$  in 1 ml DMF and 0.5 mmol  $\text{PbBr}_2$  in 1 ml DMF were injected subsequently. The yellow dispersion containing nanoparticles was directly precipitated by acetone. Finally, the nanoparticles were redispersed in toluene for use. Here the ratio between  $\text{OTABr}$  and  $\text{MABr}$  is 6:4.

**UV/Vis spectroscopy.** The ground state optical absorption spectra of the nanoparticles and bulk samples have been measured using a UV/Vis absorption spectrophotometer (PerkinElmer, Lambda 1050) equipped with integrated sphere to exclude signal from light scattering. Steady-state photoluminescence was measured using a standard spectrometer (Horiba, Spex 1681) with the excitation at 410 nm.

**TEM.** The morphology of NPs has been characterized by using a high resolution analytical transmission electron microscopy (HR-TEM) (JEOL 3000F equipped with Oxford SDD x-ray analyzer). Samples were prepared by directly depositing the NP suspension onto the carbon grid.

**FTIR.** The FT-IR measurement was conducted at Beamline D7 in MAX IV Laboratory (Sweden). For sample preparation, MCs and NPs were diluted with KBr, and were pelletised. The distance between the light source and the sample was held constant (25 cm).

**XRD.** X-ray diffraction (XRD) was used to study the crystal structure of the NPs and bulk samples. XRD was measured at Beamline I711 in MAX IV Laboratory (Sweden). The energy of the X-ray is 12.5 keV. For sample preparation, bulk sample was first annealed on a glass substrate, and then scratched off and grinded as powder to fill a glass capillary. Colloidal NP sample was mounted in a glass capillary and then put in vacuum to slowly evaporate the solvent. The glass capillaries are with the outer diameter 0.5 mm, and wall thickness 0.01 mm. The XRD patterns are measured in the transmission mode. The MAUD software was used for determining the lattice properties and crystal structures through Rietveld refinement.

**XAS.** Extended X-ray absorption fine structure (EXAFS) spectroscopy and X-ray absorption near edge structure (XANES) spectroscopy have been used to study the bonding and charge environment in the NPs and bulk samples. EXAFS and XANES were performed at Beamline I811 in MAX IV Laboratory (Sweden). XANES was measured at both Br-K and Pb-L3 edges. Due to the close location of the absorption edges of Pb-L3 and Br-K, the EXAFS can be only measured at Br-K edges. For measurement, bulk sample are annealed onto the Kapton film. Colloidal NPs with the appropriate concentration are directly deposited on to the Kapton film and the solvent evaporated in vacuum. Measurements were conducted in total fluorescence mode. The possibility of self-absorption of the sample was carefully ruled out, through identical XAS spectra measured in total fluorescence mode, transmission mode, and total electron yield. For each measurement, five scans were recorded. Raw data were corrected and converted to wavevector ( $k$ ) space EXAFS function  $\chi(k)$ , and then to Fourier transform ( $R$ ) space function  $\chi(R)$  by multiplying a Hanning window using Athena program. In  $k$ -space, the data were weighted by  $k^2$  to enlarge the oscillations at high  $k$ . The data were fitted using program Artemis with FEFF 6.0. The input structure was the Rietveld refinement result of the XRD measurement.

**XPS.** X-ray photoelectron spectroscopy (XPS) measurements were performed at beamline D1011 at MAX IV Laboratory, with normal emission geometry. The photon energy was tunable within 200-1000 eV, in order to achieve different escape depth underneath the surface. The energy scale in the spectra was calibrated relative to Fermi level by using a gold foil which was put in electrical contact with the sample. Multiple positions on the sample were measured to prove the homogeneity of the film. At each position, more than twenty scans were recorded and compared. No charging or beam-induced sample decomposition effects were detected in the spectra. The bulk samples were deposited onto fluorine doped tin oxide (FTO) glass substrate by drying the solution of the equimolar mixture of MABr and PbBr<sub>2</sub> at 85°C. The NPs were deposited on to FTO substrate by evaporating the solvent in the vacuum.

## **2. Comparison of simulated XRD patterns**

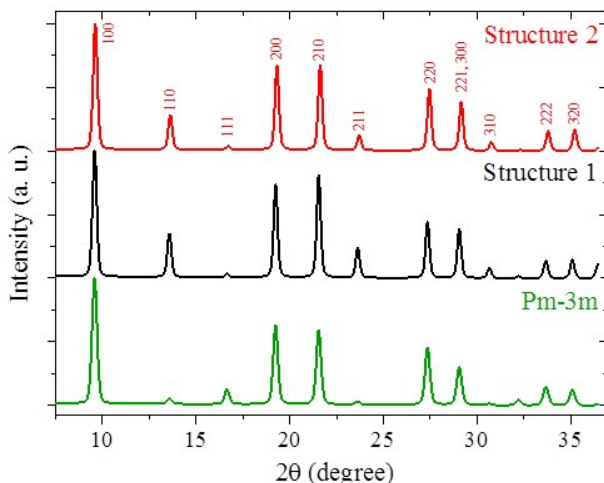


Figure S1. Comparison of the calculated XRD patterns based on three structures: standard cubic Pm-3m space group, <sup>1</sup> Structure 1 – pseudocubic P4mm space group with Pb-Br1-Pb distorted, and Structure 2 - P4mm space group with undistorted Pb-Br1-Pb bonding. Both Structure 1 and 2 are elaborated in the main text. The calculation results on Structure 1 and 2 correspond very well to the experimental results of MCs and NPs, respectively. The calculated Pm-3m XRD pattern resembles neither of the two experimental curves, known from peak (111) and (211), which justifies that the lattice in MCs and NPs are P4mm rather than the perfect cubic Pm-3m space group that are usually published for single crystal MAPbBr<sub>3</sub>.

### 3. Rietveld refinement of XRD of MCs

The input structure for fitting is from the MAPbI<sub>3</sub> with space group P4mm in Ref. <sup>2</sup>, where I is replaced manually by Br. The Rietveld refinement is done by using MAUD. The z positions of Pb, Br1, and Br2 were fitted using the profiles and intensities of 11 diffraction peaks, 2\*theta from 7 to 38 degree, shown in Fig. 3 (a). All the statistical errors that value the quality of the fitting are listed below:

- Rwp: 0.091378696
- Rp: 0.071565494
- Rwpnb (no background): 0.13626881
- Rwpnb1 (no bkg rescaled): 0.10063939
- Rwpnb2 (no bkg rescaled<sup>2</sup>): 0.08573719
- Rpnb (no background): 0.12952146
- Rpnb1 (no bkg rescaled): 0.08939369
- Rpnb2 (no bkg rescaled<sup>2</sup>): 0.07198524

### 4. Bond distances and angles in Structure 1 and 2 from XRD analysis.

Table S1 Bond distances and angles in Structure 1 and 2

Bond Lengths (Å)	Structure 1	Structure 2
Pb-Br1	2.9780(10)	2.9491
Pb-Br2	2.7785(9)	2.7788
Pb-Br2	3.1305(11)	3.1195
Bond angles (°)	Structure 1	Structure 2
Br1-Pb-Br2	83.577(8)	90.00
Br1-Pb-Br2	96.423(8)	90.00
Br1-Pb-Br1	89.283(7)	90.00
Br1-Pb-Br1	167.153(8)	180.00
Br2-Pb-Br2	180.00	180.00
Pb-Br2-Pb	180.00	180.00
Pb-Br1-Pb	167.153(8)	180.00

The standard deviations shown in parentheses of Structure 1 come from structural refinement of the experimental XRD of MCs.

### 5. Calculation of the equivalent hydrostatic pressure in NPs from lattice compression

The equivalent hydrostatic pressure from lattice compression can be estimated based on the expression of bulk modulus:  $B = -V(dP/dV)$ , where  $P$  is the pressure, and  $V$  is the volume of the unit cell. This famous Murnaghan equation for estimating the hydrostatic pressure is based on the assumption that the bulk modulus is a linear function of pressure.<sup>3</sup> The calculation requires the value of bulk modulus derivative  $B'$ , that has not been published for MAPbBr<sub>3</sub> yet. To simplify the problem, we assume that the bulk modulus is constant within 3.5% lattice compression. We use only the parameter  $B$  and lattice constants before and after compression, to roughly estimate the pressure experienced by the lattice in NPs. With the calculated  $B$  value for MAPbBr<sub>3</sub> single crystal in,<sup>4</sup> the pressure in NPs is estimated to be 0.3 GPa corresponding to the 3.5% lattice compression with respect to MCs.

### 6. EXAFS of MCs

Taking the structure shown in Fig. 3(b) as a starting point, the short range order: Pb-Br-Pb bonding of MCs, has been studied by using EXAFS at Br-K edge. Fig. S2 displays the XAS spectrum, EXAFS oscillations  $k^2\chi$ , and the Fourier transform (FT) of MCs at Br K edge. The FT result was fitted by using the theoretical amplitude and phase shift functions generated with FEFF 6 code based on the first coordination shell of the refined atomic structure obtained from XRD. The first coordination shell in the samples under examination is composed by 2 Pb nearest-neighbors, while three Br centers: 1 Br1 and 2 Br2 (shown in Fig. 3 (b)) were fitted simultaneously as the central atoms. The fitting results indicate that the twin peaks at 2.65 and 3.21 Å in Fig. 4(c) are both from the Br-Pb bonding after phase correction:  $R_{\text{Br1-Pb}}$  is fitted to be 2.924 Å, with the Debye-Waller

factor  $0.0188 \text{ \AA}^2$ .  $R_{\text{Br2-Pb}}$  was fitted to be 2.627 and 3.067  $\text{\AA}$ , with the Debye-Waller factor is  $0.0309 \text{ \AA}^2$ . This is an additional evidence for the non-perfect octahedral coordination.

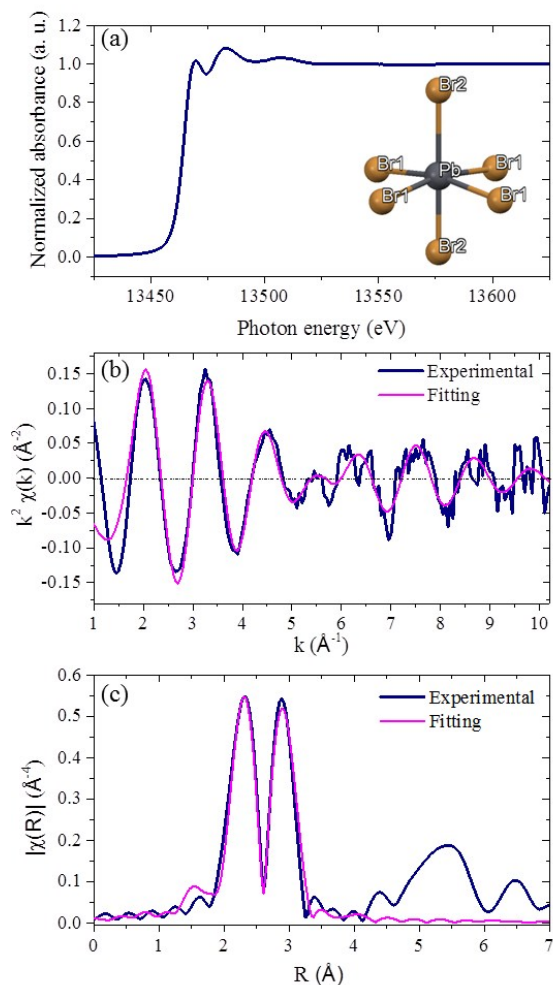


Figure S2 The magnitude of the Fourier transformation of the EXAFS oscillations and the best fit of the first coordination shells for  $\text{MAPbBr}_3$  bulk sample. The fitting analysis was carried out in the complete range of  $k=1-10 \text{ \AA}^{-1}$  and  $R=2-3.2 \text{ \AA}$  using Hanning window function. (a) The Br-K edge absorption spectra of MCs. (b) the  $k^2$ -weighted EXAFS oscillation and the simulation result. (c) Fourier transform amplitudes of the EXAFS  $k^2\chi$  data together with the simulation result. (Inset) The structural motif used in the simulation.

## 7. Structure 2 composed by the proposed motif for NPs:

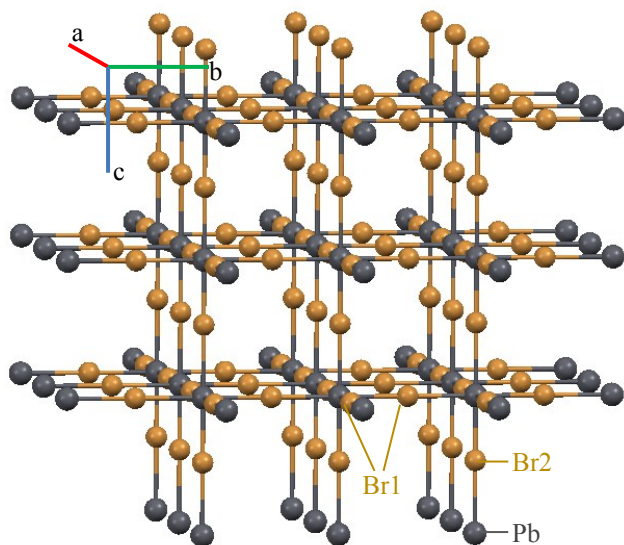


Figure S3 Lattice framework based on the proposed crystal structure of NPs (named as Structure 2). The relative atomic coordination of Pb and Br2 are the same as in the structure of MCs (Structure 1), while the position of Br1 is changed to make Br1-Pb-Br1 angle equal to  $180^\circ$

## 8. Photoionization cross-sections

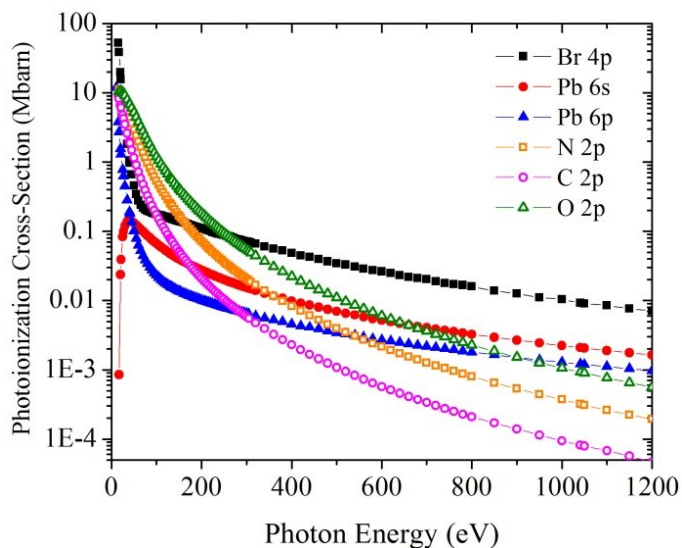
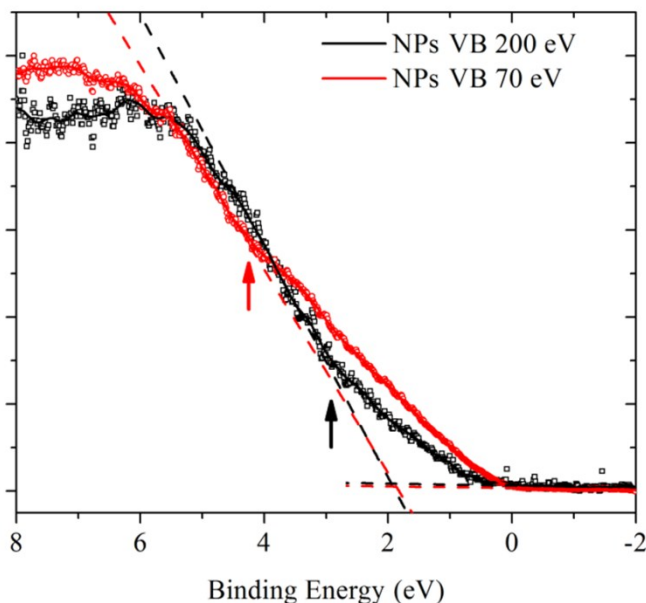


Figure S4. The photoionization cross-sections of possible contributing orbitals to VB spectra versus photon energy,<sup>3-4</sup> the data shown here are those calculated in the dipole length approximation.<sup>5</sup>

## 9. VB of NPs characterized at PEEM:

The VB of NPs measured by XPS at PEEM end-station of Beamline I311 of MAX IV laboratory (Sweden) with two different X-ray energies, 200 eV and 70 eV, in Fig. S6. The sample preparation was the same as for the XPS measurements. We pick the main NPs phase without any 2D nanoplates in the probe. The lineshape of the valence band is consistent with the XPS spectra in Fig. 7a of the main text, which indicate they represent the feature from main NPs. In addition, the escape depth corresponding to the valence electron emission are 8 Å and 5 Å for 200 eV and 70 eV photon energy, respectively, based on the calculation results of PbS powder.<sup>6</sup> Both VB spectra display extra components at lower binding energy, seen from obviously different slopes. At photon energy 70 eV, this extra component is greatly increased compared with the spectra at 200 eV, which means that this component is related to the surface of the sample.



**Figure S5. VB of NPs measured by XPS with two different X-ray energies: 200 eV (black) and 70 eV (red).**

### Reference:

1. Mashiyama, H., Kawamura, Y. & Kasano, H. Disordered Configuration of Methylammonium of  $\text{CH}_3\text{NH}_3\text{PbBr}_3$  Determined by Single Crystal Neutron Diffractometry. *Ferroelectrics* **348**, 182–186 (2007).
2. Stoumpos, C. C., Malliakas, C. D. & Kanatzidis, M. G. Semiconducting tin and lead iodide perovskites with organic cations: phase transitions, high mobilities, and near-infrared photoluminescent properties. *Inorg. Chem.* **52**, 9019–38 (2013).
3. Murnaghan, F. The compressibility of media under extreme pressures. *Proc. Natl. Acad. Sci.* **30**, 244–247 (1944).

4. Chang, Y., Park, C. & Matsuishi, K. First-Principles Study of the Structural and the Electronic Properties of the Lead-Halide-Based Inorganic-Organic Perovskites (CH<sub>3</sub>NH<sub>3</sub>)PbX<sub>3</sub> and CsPbX. *J. Korean Phys. Soc. Phys. Soc.* **44**, 889–893 (2004).
5. Yeh, J. & Lindau, I. Atomic subshell photoionization cross sections and asymmetry parameters:  $1 < Z < 103$ . *At. data Nucl. data tables* **32**, 1–155 (1985).
6. Tanuma, S.; Powell, C. J.; Penn, D. R. *Surf. Interface Anal.* **2011**, *43*, 689-713.